UDC 004.681.2.08

A.I. Guda, A.Yu. Zimoglyad

BUCK CONVERTER SIMULATION AND MEASUREMENT

Abstract. For thermal evaporation of metal in vacuum, was needed adjustable power source capable of delivering a sufficiently high current (usually 25-50 A) and a low voltage of 1-5 Volts. This source is needed to heat the boiling type evaporator of molybdenum or titanium, resistance of which can be from 0.05 - 0.5 Ohm.

To conduct research in the field of creating functional coatings, mentioned in [3,4], was required a mathematics model of buck converter. Without correct model is practically impossible to build adjustable power source for thermal evaporation of metal in vacuum.

Keywords: step down DC/DC converter, buck, vacuum evaporation.

Introduction

Buck (or "step-down") converter is one of the most usable approaches to get controlled power source with lesser voltage and higher current, then original power source. Modern components allow as to achieve outstanding power conversion coefficient and minimal mass and size in comparison with classic low frequency transformer-based approach. Nevertheless, this converter has less obvious characteristics, especially in situations, where large output voltage range, precision output or fast reaction is required. Some of these requirements can be fulfilled by correctly designed feedback, but, in turn, this design requires adequate model of the converter itself.

One of the possible simplified schematic realization is shown in the fig. 1, where: V_{cc} – external voltage source, V_2 – output voltage, R_h – load, L – inductive element, which have essential role in conversion, C_2 – output capacitor. Input capacitors C_1 is often not the separated element of the schematics. It can be represented by inner capacitance of the diode, and/or as a part of the snubber branch. Without it a correct modeling is practically impos-

sible, as if the both switches of half-bridge is closed, it is no way to determine V_1 – voltage on left inductor foot.
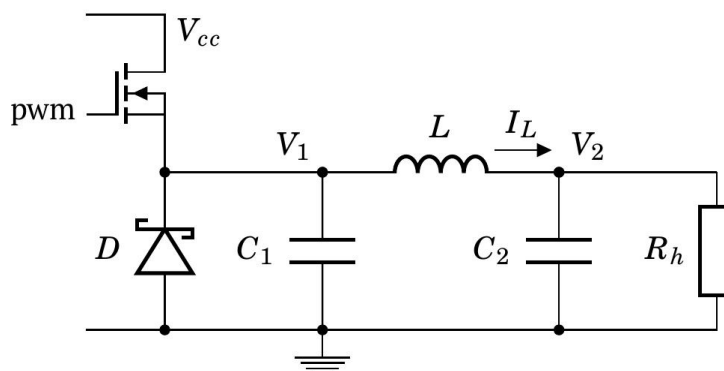

Figure 1 –Buck converter schematics with Schottky diode in bottom part

Half-bridge part, which conducts switching discipline for the inductive element L, requires two switches. Upper part may be represented by MOSFET (as shown in figure), BJT or IGBT transistors. This part is controlled by the PWM signal source. Lower part may be represented as by other transistor, with own control signal, or by passive switching element, like Schottky diode. Schematics with two transistors can give as higher conversion coefficient, but require more complex control, especially if wide output range is required. Large voltage drop on Schottky diode leads to smaller power conversion coefficient, but requires no additional control, and schematic with it can operate in different modes.

Input PWM frequency f_{pwm} defines full control period T_0, whereas time T_1, where upper switch is open, defines duty cycle γ :

$$T_0 = \frac{1}{f_{pwm}}, \quad \gamma = \frac{T_1}{T_0}, \quad \gamma \in [0,1). \tag{1}$$

Main part

Buck converter common model

For the first approximation, we assume, that most of the element is ideal, i.e. $V_{cc} = const$, $L = const$, MOSFET in closed state characterized by infinite resistance, in open state is equivalent of small ordinary resistor, and switching is instantaneous. In such assumptions the model dynamics is defined by the next equations system:

$$\begin{cases} C_1\dot{V_1} = \dfrac{\text{pwm}(t)(V_{cc}-V_1)}{R_{ch}} + I_d(V_1) - I_L, \\[2mm] L\dot{I_L} = V_2 - V_1, \\[2mm] C_2\dot{V_2} = I_L - \dfrac{V_2}{R_h}, \\[2mm] I_d(V) = I_s\left(\exp(\dfrac{V}{N_d V_t}) - 1\right). \end{cases} \quad (2)$$

where $\text{pwm}(t)$ – PWM signal (0 or 1), R_{ch} – net resistance of the charging branch, composed from MOSFET channel resistance in open state, serial resistance of capacitors in power source and so on, $I_d(V_1)$ – current via Schottky diode, R_h – load (heather) resistance (counting wires resistance), I_s, N_d, V_t -- Schottky diode parameters. Other values are denoted in the fig. 1.

In spite of simplicity, numerical solutions of this system in real conditions have some difficulties. First of all, an extremely different time scale co-exists in this context. The typical value of R_{ch} constitutes $10m\Omega$., and $C_1 \approx 10^{-10}\text{F}...10^{-8}\text{F}$. Consequently, the required time step in numerical calculation can be as less as 10^{-12}s. On the other side, the values of C_2 is often much greater, and required full simulation time can reach $10^{-2}...10^2\text{s}$. This lead to really huge number of the simulation steps, and wast amount of memory, if we need full process history. Nevertheless, to determine possible methods of diminishing amount of calculations, a series of the numerical simulations of some typical cases was conducted.

The values of the schematic components was selected with respect to real equipment, that was used in vacuum thermal evaporation process. So, we assume, that $V_{cc} = 12\text{V}$, $f_{\text{pwm}} = 100\text{kHz}$, $C_1 = 10n\text{F}$, $C_2 = 6600\mu\text{F}$, $L = 1e-5\text{H}$, $I_s = 2.42\cdot10^{-5}\text{A}$, $N_d = 1.78$, $\gamma \in [0.02;0.7]$, $R_h \in [0.1;10]\,\Omega$.

Using these parameters, it is possible to compose a pack of dimensionless values. The most valuable of them is based on the relations of the time-based expressions to PWM period T_0. So, we define:

$$\beta_{LRh} = \frac{L}{R_h T_0}, \quad \beta_{C1Rch} = \frac{C_1 R_{ch}}{T_0}, \quad \beta_{C2Rh} = \frac{C_2 R_h}{T_0}, \quad \beta_{C1L} = \frac{\sqrt{C_1 L}}{T_0}, \quad \beta_{C2L} = \frac{\sqrt{C_2 L}}{T_0}. \quad (3)$$

In the conditions, described above, we receive:

$\beta_{LRh} \in [0.1...10]$, $\beta_{C1Rch} = 10^{-5}$, $\beta_{C2Rh} \in [66...\ 6.6\cdot10^3]$, $\beta_{C1L} \approx 3.16\cdot10^{-2}$, $\beta_{C2L} \approx 26$.

Extremely low value of β_{C1Rch} emphasises fact, that processes of C_1 charging and discharging may be neglected in simulation. In this condition, a correct $V_1(t)$ definition must be provided. The values of β_{C1L}, β_{C2L} have no visible representation in this schematics, as oscillations is not a intended operation mode.

Using the give R_h range, we receive values of β_{LRh} and β_{C2Rh} both greater and less then 1. This means, that we have different operation modes. Really, the proper value of R_h, which can give us reasonable power, is much more strict: $R_h \in [0.1; 0.5]\,\Omega$. So in the case of $R_h = 0.5\Omega$ we get $\beta_{LRh} = 2$ (this means, that that inductive process on L -- R_h branch have the same order with T_0, but still some slower). And $\beta_{C_2 R_h} = 3.3 \cdot 10^2.$, which we really can ignore $V_2(t)$ changes during one PWM cycle.

In the fig. 2 the simulation results with given set of parameters $\gamma = 0.1$, $R_h = 0.5\Omega$, $V_2(0) = V_{20} = 0$ V, $I_L(0) = I_{L0} = 0$ are presented.

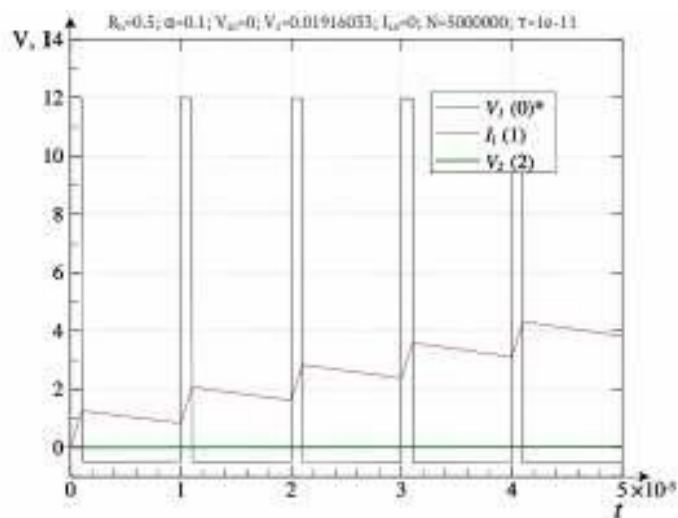Figure 2 – Buck converter simulation: $\gamma = 0.1$, $R_h = 0.5\Omega$, $V_{20} = 0$V, $I_L(0) = I_{L0} = 0$

To receive this result, it was required 5000000 simulation steps, $1 \cdot 10^{-11}$s (τ) each. If time step was increased to 10^{-10}s, simulation process became unstable, and infinite result was detected. Nevertheless, the results plot is simple, without complex behaviour. The only value, which shows fast changes, is $V_1(t)$ – sharp square plot appears a well-known charging curve only at the time scale near to 10^{-9}s. The state is far from stable condition, as $I_L(t)$

increases after each PWM period. The V_2 value is increases too, but, due to large $\beta_{C_2 R_h}$ value, this change can be neglected during one PWM period (T_0). So, in this condition, each PWM period can be divided into two parts. On each part both $I_L(t)$ and $V_2(t)$ dependencies are near to linear. The $V_1(t)$ dependency in the visible time scale have 2 values: near V_{cc} if $\mathrm{pwm}(t) = 1$, and $V_{dn} \approx -0.48\mathrm{V}$ (Schottky diode open voltage) otherwise. These facts may significantly decrease model complexity, and, consequently, amount of the required computational resources.

In the fig. 3 the simulation results with similar set of parameters $\gamma = 0.1$, $R_h = 0.5\Omega$, $V_{20} = 0.79\mathrm{V}$, $I_{L0} = 1.07A$ are presented. The main difference with previous figure is that an initial condition was selected to provide quasi-stationary behaviour. But the main result is the same: each PWM period can be divided into two simple parts.
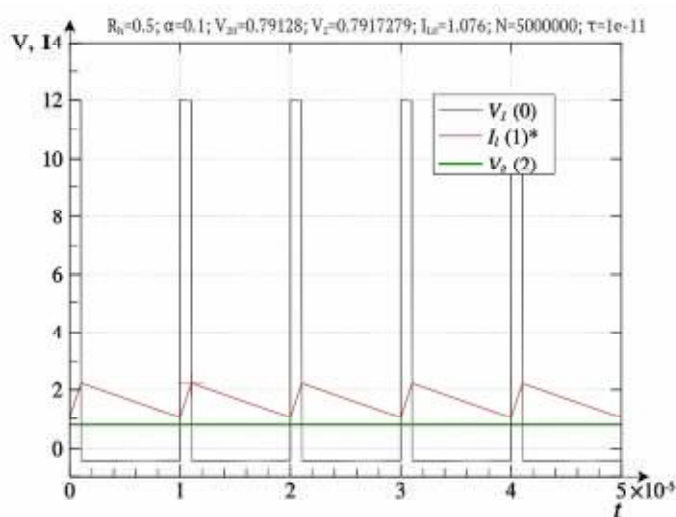

Figure 3 –Buck converter simulation: $\gamma = 0.1$, $R_h = 0.5\Omega$, $V_{20} = 0.79\mathrm{V}$, $I_{L0} = 1.07\mathrm{A}$

The fig. 4 shows some different result. The initial conditions was selected to be near to stationary too ($\gamma = 0.1$, $R_h = 5\Omega$, $V_2(t) = V_{20} = 1.32\mathrm{V}$), but model demonstrates more complex behaviour. First of all, there is at least 3 parts in every PWM period. First and second show similar behaviour with previous cases, but the magnetic flux in inductor is not strong enough to support continuous current. This mode is known as ``discontinuous conduction mode'' (DCM). Moreover, in this part of period we can observe $V_1(t)$ and $I_L(t)$ oscilla-

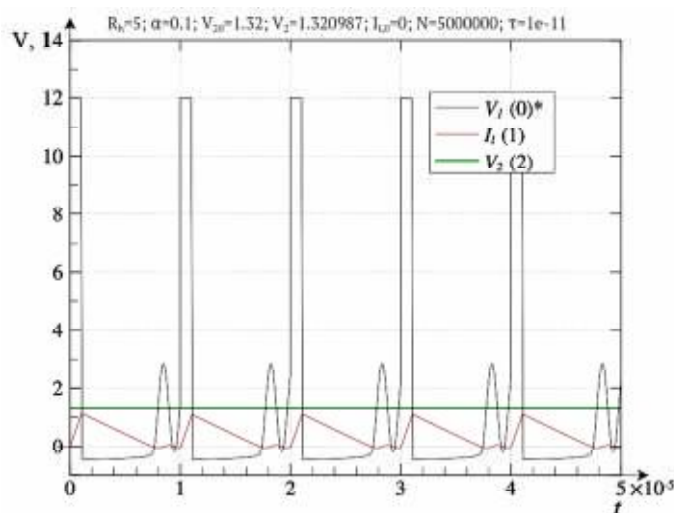tions, but in real schematics it can be suppressed by snubber and other approaches.

Figure 4 – Buck converter simulation: $\gamma = 0.1$, $R_h = 5\Omega$, $V_{20} = 1.32\text{V}$

This division in 3 parts is not observed, if active element is used in bottom part of half-bridge. But in this case we may receive alternative current in inductor, which is not a desirable mode for most purposes.

Buck converter simplified model

As it was previously mentioned, if $\beta_{C1Rch} \ll 1$, and other dimensionless values not, the equation (\ref{atu:eq:buck_dyn1}) may be simplified. In this case $V_1(t)$ must be given. To define this values, we can use the fact, that in used conditions there is 3 characteristic values: near the V_{cc}, if $\text{pwm}(t) > 0$, V_{dn} or zero otherwise. So, the equations system becomes:

$$
\begin{cases}
L\dot{I}_L = V_2 - V_1(t), \\
C_2\dot{V}_2 = I_L - \dfrac{V_2}{R_h}, \\
V_1(t) = \begin{cases}
V_{cc} - R_{ch}I_l, & \text{pwm}(t) > 0, \\
V_{dn}, & \text{pwm}(t) = 0, I_L > 0, \\
0, & \text{pwm}(t) = 0, I_L = 0
\end{cases}
\end{cases}
$$

(4)

This model required additional schematic limitation: $I_L(t) \geq 0$.

The simulations results in the conditions, equal to the first simulation (fig 2), is shown in the fig. 5.
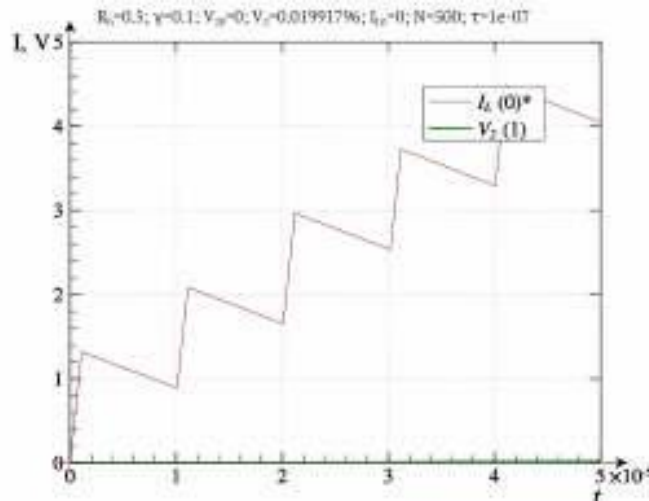

Figure 5 – Buck converter simplified simulation: $\gamma = 0.1$, $R_h = 0.5\Omega$, $V_{20} = 0V$, $I_L(0) = I_{L0} = 0$

The simulation results is quite near and other simulations shows similar results. The prominent difference is the τ value: the first model requires minimal values about 10^{-11}, whereas simplified model requires 10^{-7}, so calculation is 1000 times faster, and requires less memory to store results.

Using this model, the $V_2(R_h, \gamma)$ dependencies was received in the case of fixed this and other similar values.

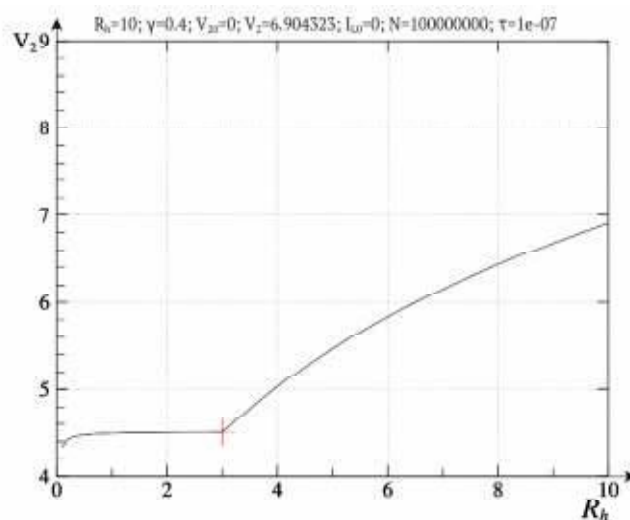In the figure 6 the final simulations results are presented as $V_2(R_h)$ dependency for fixed γ.

Figure 6 – $V_2(R_h)$ dependency for $\gamma = 0.4$

The plot is dived into 3 parts: central part corresponds continuous mode, where output voltage is practically independent from load, left part demonstrates voltage drop under high load, and right part corresponds to discontinuous mode.

In the figure 7 simulations results are presented as $V_2(R_h, \gamma)$ dependency.
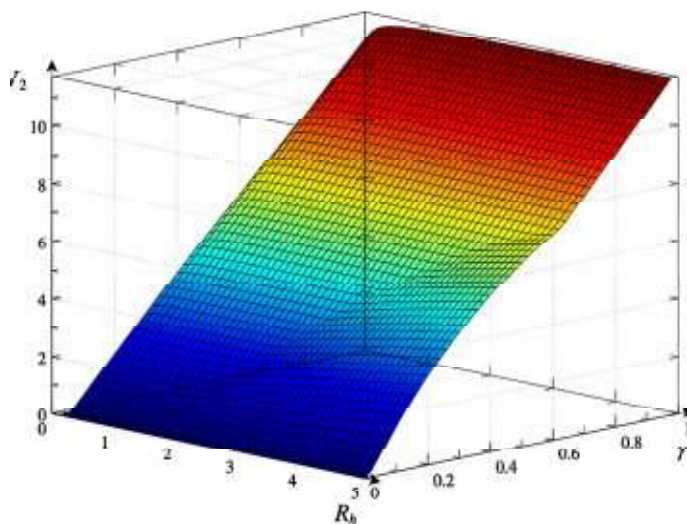

Figure 7 – $V_2(R_h, \gamma)$ dependency

The results show, that to achieve near to linear dependency $V_2(\gamma)$, the continuous mode must be used. If R_h range is not to large, than in near to steady conditions this may be fulfilled by correct chaise of the L, f_{pwm} values. Discontinuous can not be avoided, if γ changes rapidly, but this state is transient.

In the continuous mode effective output resistance is given as $R_s = R_{ch}\gamma$, so at low γ this power source can drive low-resistance load without essential voltage drop.

Quasi-steady state

Previous simulations shows, that in typical conditions there is 3 different time scale for the processes in buck converter. The first – C_1 charging and discharging, characterized by time scales $10^{-11}...10^{-9}s$. Next scale – $10^{-6}...10^{-4}s$, which is corresponding to f_{pwm} and fast current changes in inductor. The third scale – $10^{-3}...10^{2}s$ corresponds to C_2 charging and discharging processes. In

this scale changes is conditioned by the changes of the load resistance, PWM parameters, or initial conditions. If these values are fixed at constant level, we assume, converter is in the quasi-steady state, as changes are occurring in first and second time scale levels. For the simplicity, we will denote this situation as simple ``steady state'', counting for limitations.

In this steady state:

$$\dot{V_2} \approx 0, I_L(t) = I_L(t + n \cdot T_0). \tag{5}$$

Let $V_{cc} \gg |V_{dn}|$, $V_{dn} \approx -0.48\text{V}$. As for zero approximation, we assume, that $I_L R_{ch} \ll V_{cc}$.

The schematic pictures for one PWM cycle is represented in fig 8, continuous (a) and discontinuous (d) mode accordingly.
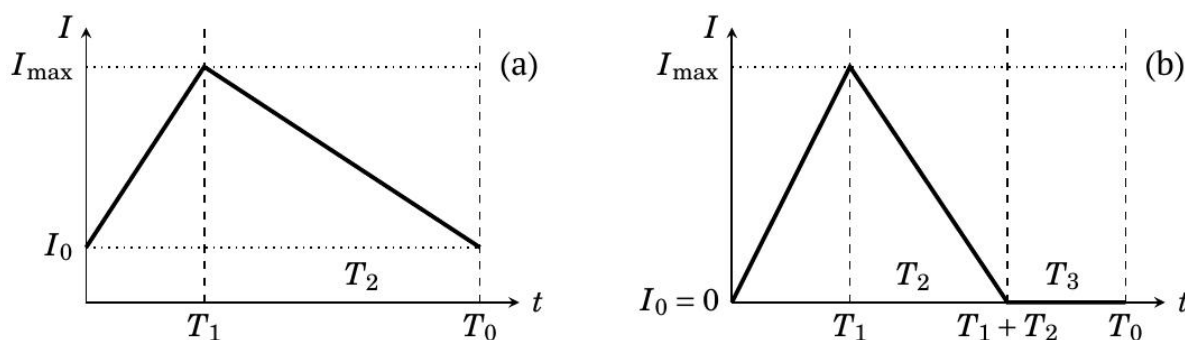

Figure 8 – Simplified dependencies $I_L(t)$ for continuous (a) and discontinuous (b) modes

In continuous mode $T_0 = T_1 + T_2$, $I_0 \geq 0$.

$$I_{\max} = I_0 + \frac{T_1}{L}(V_{cc} - V_2) = I_0 + \frac{T_2}{L}(V_2 - V_{dn}). \tag{6}$$

$$V_2 = V_{cc}\frac{T_1}{T_0} + V_{dn}\left(1 - \frac{T_1}{T_0}\right) = V_{cc}\gamma + V_{dn}(1 - \gamma). \tag{7}$$

The equation~(\ref{atu:eq:buck_V_2}) is often simplified as

$$V_2 \approx V_{cc}\gamma,$$

but for low γ values this will lead to essential errors. On the other side, equation~(\ref{atu:eq:buck_V_2}) gives wrong (< 0) results low γ values, bus in this case CCM condition is not fulfilled.

As we can see, the values of I_0, R_h are not appears in this calculation, so balance point is independent of load in this case. But there still exist limitation: $I_0 \geq 0$. Therefore, we can determine I_0, using the charge balance:

$$q_{in} = T_0 I_0 + \frac{T_0 T_1}{2L}(V_{cc} - V_2) \approx T_0 I_0 + \frac{T_0^2 \gamma V_{cc}}{2L}(1-\gamma), \tag{8}$$

$$q_{out} = T_0 \frac{V_2}{R_h} \approx \frac{T_0 V_{cc} \gamma}{R_h}. \tag{9}$$

$$I_0 = \frac{V_{cc}\gamma}{R_h} - \frac{T_0 \gamma V_{cc}}{2L}(1-\gamma) = V_{cc}\gamma\left(\frac{1}{R_h} - \frac{T_0(1-\gamma)}{2L}\right) = \frac{V_{cc}\gamma}{R_h}\left(1 - \frac{T_0 R_h (1-\gamma)}{2L}\right). \tag{10}$$

The condition for continuous mode becomes:

$$\frac{T_0 R_h (1-\gamma)}{2L} \leq 1, \quad \text{or} \quad \gamma \geq 1 - \frac{2L}{T_0 R_h} = \gamma_{crit}. \tag{11}$$

In discontinuous mode condition $I_L(0) = I_L(T_0) = 0$ fulfilled automatically, so it is impossible to determine V_2 from this equation.

$$\frac{T_0 \gamma V_{cc}}{2L}(1-\gamma), \tag{12}$$

$$I_{max} = \frac{T_1}{L}(V_{cc} - V_2) = \frac{T_2}{L}V_2, \tag{13}$$

$$q_{in} = \frac{T_1^2}{2L}(V_{cc} - V_2) + \frac{T_2^2}{2L}V_2. \tag{14}$$

$$q_{out} = \frac{T_0 V_2}{R_h}. \tag{15}$$

Solving simultaneously:

$$\begin{cases} T_1 V_{cc} - T_1 V_2 - T_2 V_2 = 0, \\ T_1^2 V_{cc} - T_1^2 V_2 + T_2^2 V_2 = 2T_0 L V_2 / R_h, \end{cases} \tag{16}$$

we receive:

$$T_2 = -\frac{sqrt R_h^2 T_1^2 + 8LR_h T_0 + R_h T_1}{2R_h}, \quad V_2 = -\frac{T_1 sqrt R_h^2 T_1^2 + 8LR_h T_0 V_{cc} + R_h T_1^2 V_{cc}}{4LT_0}, \tag{17}$$

$$T_2 = \frac{sqrt R_h^2 T_1^2 + 8LR_h T_0 - R_h T_1}{2R_h}, \quad V_2 = \frac{T_1 sqrt R_h^2 T_1^2 + 8LR_h T_0 V_{cc} - R_h T_1^2 V_{cc}}{4LT_0}$$

$$T_2 = -\frac{T_1}{2} + \frac{1}{2R_h} sqrt R_h^2 T_1^2 + 8LR_h T_0 = -\frac{T_0 \gamma}{2} + \frac{1}{2} sqrt T_0^2 \gamma^2 + 8LT_0 / R_h = \frac{T_0}{2}\left(sqrt \gamma^2 + 8\beta_{LRh} - \gamma\right).$$

This calculations is in good correspondence with the results, shown in previous section, so may be used in the cases, where fast dynamics of R_h and γ is not observed.

Comparison with real converter

The series of the real equipment experiment was conducted to verify simulations results. Real buck converter from the thin metal film creation in the vacuum device was investigated. At some fixed γ values dependencies $V_2(R_h)$ was acquired. Then, quasi-steady approach was used, taking into account additional voltage drop. The results in show in the fig 9.
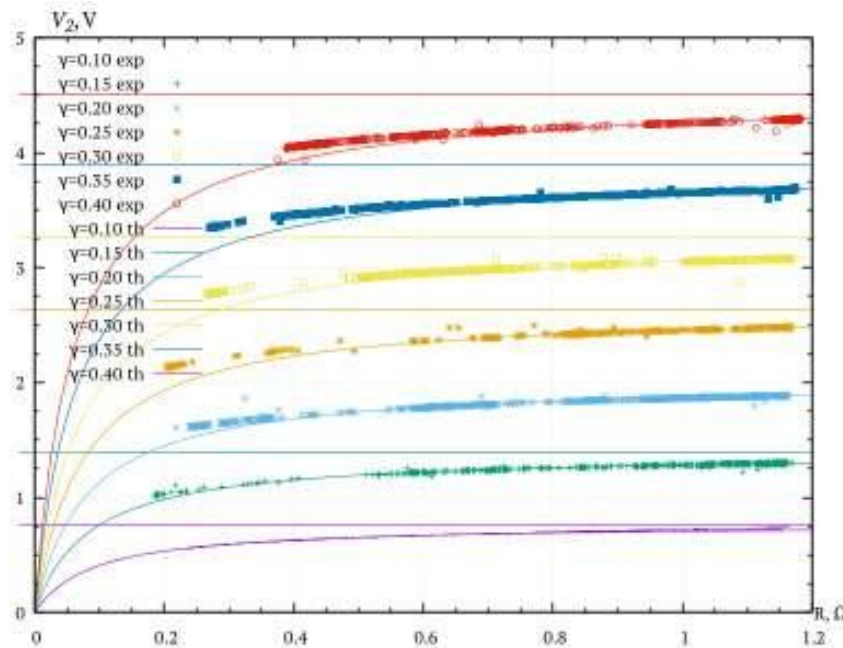

Figure 9 – Real and model $V_2(R_h, \gamma)$ dependencies

The difference between real experiment and quasi-steady model can be neglected in most ranges, except extremely high load. Nevertheless, this power source gives us practically better results, than theory.

Conclusions

Taking into account all mentioned calculations, simulations and measurements, the following conclusions can be made:

– The (1) equation can describe many features in the buck converter behaviour, but numerical simulation requires wast amount of the computational resources in this case.

– In many practical cases, it may be possible to use equation system (2), which requires up to 10^4 times less resources, but still give us adequate results.

– Quasi-state approach gives us correct analytical results, which can be used in simulations, where R_h and γ changes slowly.

– Comparison with data, acquired in real experiment, confirms correctness of the proposed models and methods.

REFERENCES

1.   Steve Roberts DC/DC book of knowledge / Steve Roberts // RECOM Group Gmunden 2014. – 234 p.

2.   Mattox Handbook of Physical Vapor Deposition (PVD) Processing: Film Formation, Adhesion, Surface Preparation and Contamination Control / Mattox, M. Donald // Westwood, N.J.: Noyes Publications, 1998 — 944p.

3.   Mikhalev A.I. Modelirovaniye fraktalnykh struktur funktsionalnykh pokrytiy s uchetom skorosti napyleniya / Mikhalev A.I., Guda A.I., Zimoglyad A.YU. Kovtun V.V. //Vísnik KHNTU -2018.- №3(66) S.- 115-120

4.   Zimoglyad A.YU. Yssledovanye zavysymosty koeffytsyenta trenyya metallycheskykh plenok ot fraktalnoy razmernosty / Zimoglyad A.YU., Guda A.Y., Kovtun V.V. Zhurba A.A. // Systemni tekhnolohiyi. Rehionalnyy mizhvuzivskyy zbirnyk naukovykh prats- 2018. - №2 (115) S.- 9 -13.

5.   Horovits P. The Art of Electronics / P. Horowitz, W. Hill. - Moscow: Mir, 1995. – 154p.

6.   Powell Vapor Deposition. The Electrochemical Society series / F. Carroll, H. Joseph, Oxley, J. M. Blocher // New York: Wiley, 1966— 158 p.